



Understanding performance of transmission and distribution insulators at very low temperature conditions

Sounak Nandi¹ · B. Reddy Subba¹ · Dinesh Sharma¹

Received: 4 September 2019 / Accepted: 11 May 2020 / Published online: 10 June 2020
© Springer-Verlag GmbH Germany, part of Springer Nature 2020

Abstract

Polymeric or silicone rubber insulators are extensively used for high-voltage transmission by electrical utilities due to advantageous features like lightweight, better contamination performance, etc. The performance of silicone rubber insulators exposed to low temperature conditions with continuous application of electric stress is of utmost importance as these insulators are being used under such climatic conditions in the country. In the present work, long-term experimental investigations have been conducted for 1000 h at 0 °C and for 1500 h at –20 °C with application of electrical stress to simulate near-field conditions. A special experimental arrangement has been established for the investigations. Leakage current was monitored at regular intervals, and further material evaluation techniques like Fourier transform infrared spectroscopy (FTIR), scanning electron microscopy (SEM), energy-dispersive X-ray analysis (EDAX), mechanical strength measurements, etc., were conducted before and after the experimentation to verify the surface degradation on the polymer insulators. Some interesting results obtained during the experimentation for normal and polluted conditions along with the analysis carried out are presented.

Keywords Composite insulators · High voltage engineering · Pollution · Condition monitoring

1 Introduction

Polymeric insulators are the most popularly used among the available options like porcelain, glass, etc. Some of the significant characteristics of silicone rubber insulators include its better contamination flashover performance and lightweight. The excellent flashover resistance capability of silicone rubber insulators is due to their ability to prevent the water droplets from wetting the surface or hydrophobicity property [1, 2].

Several researchers have contributed abundantly pertaining to the performance of silicon rubber insulators. Hackam et al. [3] have discussed the aspects of polymeric insulators, dealt with various testing procedures and performance evaluation. Kumagai et al. [4] and Yoshimura et al. [5] studied the effect of various stresses on the performance of composite insulators and have conducted extensive material analysis

for justifying their observation. They have also studied the hydrophobic recovery and impact of various stresses like corona and dry-band arcing on the material composition. Ilhan and Cherney [6] deals with the performance of the RTV coating on porcelain suspension insulator. El-Hag et al. [7] have shown the validity of using low frequency harmonic content of the leakage current as a diagnostic tool for identifying various phenomena like dry-band arcing and the intensity of the arc. Meyer et al. [8] presented the role of inorganic fillers that are used in composite insulators to provide resistance to tracking and erosion. It was shown that the tracking and erosion resistance to dry-band arcing depends mainly on the effective conductivity of the composite insulator formed after mixing with the inorganic fillers. The overall performance depends on the relative percentage of the filler material and the base polymer. Phillips et al. [9] indicated the mechanism of water droplet corona and temporary loss of hydrophobicity associated with the process. Shah et al. [10] and Karady [11] studied various stages of development of polymeric insulator flashover, and they identified various mechanisms occurring prior to the development of flashover arc and the processes leading to flashover. El-Kishky and Gorur [12] deals with the activity of the

✉ B. Reddy Subba
sreddy@iisc.ac.in

¹ High Voltage Laboratory, Department of Electrical Engineering, Indian Institute of Science, Bangalore 560012, India

water droplets on insulating surface under the application of electric stress. Authors [13, 14, 15] studied the performance of polymer insulators for multistress aging. Cherney et al. [16] and Farzaneh [17, 18] studied performance of composite insulators for polluted and icing conditions. Ghosh et al. [19], Cheng et al. [20] and Wilkins [21] have mainly dealt with the mechanisms of pollution flashover.

Authors [14] have made attempt to study the effect of dry conditions under UV along with electrical stress. Recently, [22] studied aging experimentation on silicon rubber insulators under arid climatic conditions, while authors [23–25] studied aging performance on polymeric insulators under multiple stresses by application of ac and dc voltages. Authors [26, 27] deals with performance of polymer insulators under extreme and low temperature conditions. Li et al. [28] deals with the progress of the development of insulating materials. Mehmet et al. [29] studied the CTI of cable joints using both experiments and simulation, while authors [30, 31] mainly focused on the development of insulator [both porcelain and silicone rubber] flashover model using COMSOL Multiphysics and condition monitoring of electrical equipment's using electromagnetic stray fields, respectively. The available literature mainly focuses on the normal or polluted environmental conditions, and very scant literature is available on the performance or evaluation of polymer insulators at low temperature conditions 0 °C and –20 °C as these conditions exist in several places in our country and elsewhere during winter. Also, the effect of pollution or contamination under low temperature needs to be studied as utilities in the country are adopting polymeric insulators at places where the temperature goes below 20°.

Hence, the present study aims to investigate the performance of polymeric insulators at zero and sub-zero (–20 °C) temperatures with extremely low humidity under normal and polluted conditions. The leakage current is measured at regular intervals for a period of 1500 h. of experimental duration. Some significant features of the leakage current were evaluated by using the fast Fourier transform (FFT), and an effort is made to correlate the electrical parameters obtained from leakage current analysis with the surface conditions of the polymeric insulators. Further surface degradation on the insulator samples is evaluated by using FTIR, SEM, EDAX and tensile strength measurements.

2 Experimental procedure

Figure 1 shows the block diagram of the experimental arrangement. The setup consists of a specially fabricated aging chamber of size 2.5 × 2.5 × 2.5 ft with arrangement for high-voltage (HV) connection and provision for leakage current (LC) measurement. In addition, the chamber is designed to accommodate UV lamps, heater and humidifier



Fig. 1 Developed multistress aging facility. 1: AC 230 Volt, 50 Hz power supply, 2: 400 Volt, 50 Hz power supply, 3: HVAC source, 4: HVAC control panel, 5: high-voltage probe, 6: current-limiting resistor 15 k Ω , 500 W, 7: high-voltage bushing, 8: aging chamber, 9: UV-protected glass, 10: shunt box, 11: NI cDAQ for LC measurement, 12: digital oscilloscope, 13: climate chamber control panel, 14: NI cDAQ data acquisition in LabVIEW environment

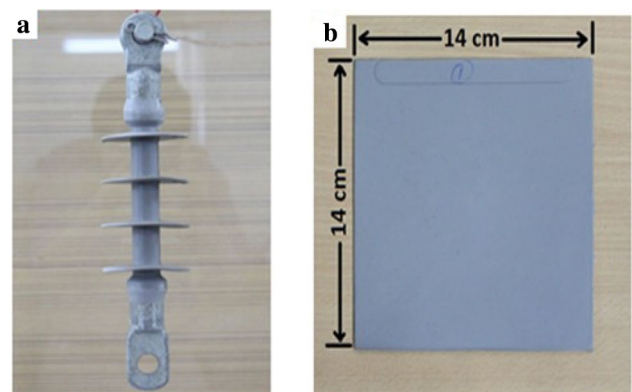


Fig. 2 a Full-scale insulator b the flat sample

to produce multiple environmental stresses simultaneously. In the present experimentation, only low temperature zero and –20 °C with ac voltage of 10 kV rms is continuously applied during the experimental duration. An HVAC source of 30 kVA with output voltage 0–30 kV rms fed with input of 400 V rms and 50 Hz power supply embedded with over voltage and over current protection for the electrical safety. A resistive shunt of 10 k Ω is used to measure the LC at the ground side by tapping the voltage across it. Source voltage and LC are monitored using RIGOL make digital storage oscilloscope DS1102E (100 MHz, 1 GSa/s).

Figure 2 shows the distribution class full-scale HTV SIR insulator samples of creepage length 347 mm and flat samples used for the study. The rated voltage is 11 kV rms line to line. Four samples of the full scale and three of the flat slab

samples are placed in the climate chamber for experimentation. Each sample is cleaned with cleaning agent (propanol) and dried in air for at least three hours, to ensure no pre-contamination which can influence the surface phenomenon. The low temperatures for the study at 0 °C and –20 °C are maintained by suitably controlling the compressors and with electric stress continuously applied for a period of 1000 and 1500 h during the period of experimental investigations.

3 Leakage current (LC) analysis

Several researchers have conducted the study and analyzed LC to find characteristics and mechanisms to monitor the surface degradation on polymeric insulators [8]. The leakage current monitoring is also used as a tool in the field to study the activity occurring on the surface of insulator from various frequency components.

Literatures available have reported the mechanism of leakage current as a process which takes place before the flashover; these reports indicate the role of water droplets and their elongation under the applied electric field is of major concern. The leakage current gives important information about the performance of insulator during the experimentation. In the present investigation, the LC was monitored continuously to study the surface conditions on the insulators. The climate chamber was maintained at very low humidity (35–40%), like the conditions exists in Leh–Ladakh region of our country.

The formation of water droplets on the surface and related phenomenon like dry-band arcing and water droplet corona was not witnessed during the experimentation. The production of leakage current is only due to some inherent conductivity of the silicone–rubber surface, this is verified on the basis of the leakage current waveform during the initial stages of the experimentation. But because singularity at the triple point could lead to increase in the electric stress, electric field enhancement at the triple junction is the main reason for the distortion of the leakage current. Very faint discharges could be seen present which were not very severe as the RMS value of the leakage current does not change considerably over the experimental period of 1500 h.

Researchers [7] have reported the presence of various harmonics in the leakage current related to some phenomenon taking place on the surface of insulator. Figure 3 represents a sinusoidal waveform which has almost no distortion. The leakage current measurements were conducted at regular intervals for both zero and sub-zero conditions for entire experimental duration. The motivation behind such experimentation is the simulation of conditions which prevail in the extreme northern portions of the country; a typical leakage current measurement conducted at 350 h at 0° conditions is presented in Fig. 3.

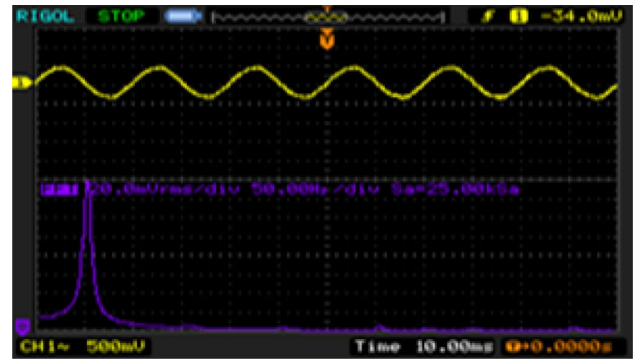


Fig. 3 Leakage current after 350 h of experimentation at 0° with electric stress applied

The leakage current waveform is nearly sinusoidal; this is due to the fact that no nonlinear phenomenon like partial arcing/discharges is taking place along the path of the leakage current. The prominent presence of fundamental component in the leakage current is an indicator that the surface is dry and shows no thermal degradation. This phenomenon was observed till for 1000 h of experimentation with only a minor increase in magnitude, and the measured peak value was about 50 microamps.

Further, it was felt necessary to extend the experimentation to the sub-zero temperature (–20°) since in winter at some places in the Country the temperature goes well below zero °C. To understand the performance of insulators at –20 °C both for polluted and non-polluted conditions, studies were conducted and the results obtained are analyzed and presented.

The experimentation is conducted at low humidity and low temperature conditions, the formation of water droplets on the surface is very low, due to this related phenomenon like dry-band arcing, water droplet corona may not occur. Leakage current is observed due to the inherent surface conductivity of the silicone rubber surface. This was verified based on the leakage current waveform during the initial stages of the experimentation. Because of singularity at the triple point near the high-voltage electrode, silicone rubber and air junction are the point of high field zone. The electric field enhancement at the triple junction is the main reason for the distortion of the leakage current. Moreover, the literature [7] reports the presence of various harmonics in the leakage current related to some phenomenon taking place on the surface. Figure 4 represents a typical sinusoidal waveform which has considerable distortion in the waveform measured after 48 h of experimentation for –20 °C with continuous voltage stress applied, and the measured peak value of leakage current is 5.8 microamps.

Figure 5 shows the leakage current waveform measured after 500 h of experimentation, and the waveform presents both the magnitude and level of distortion in the waveform

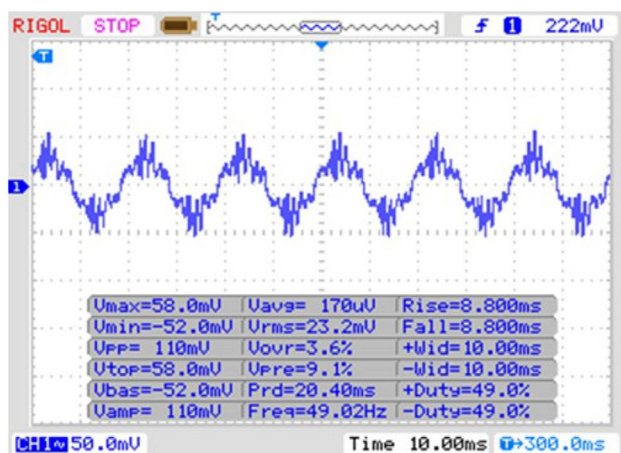


Fig. 4 Leakage current after 48 h of experimentation at $-20\text{ }^{\circ}\text{C}$

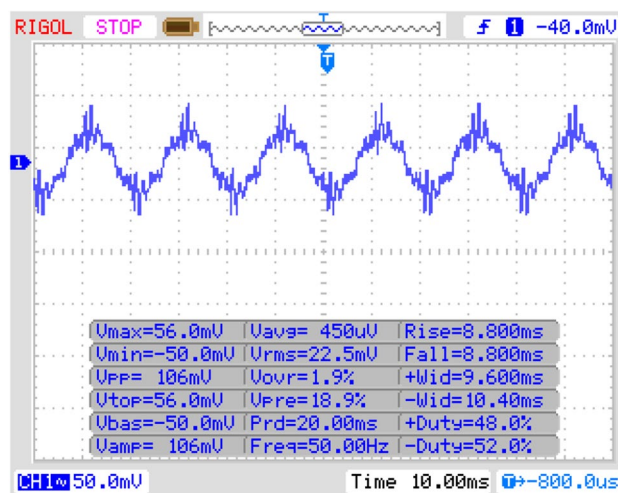


Fig. 6 Leakage current after 900 h of experimentation at $-20\text{ }^{\circ}\text{C}$

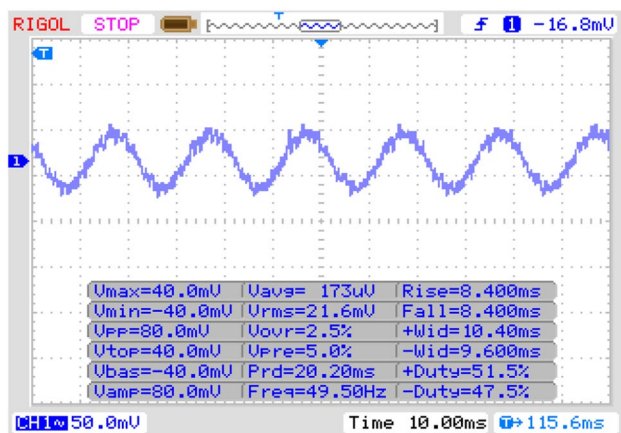


Fig. 5 Leakage current after 500 h of experimentation at $-20\text{ }^{\circ}\text{C}$

is lower. Similarly, measurements conducted at 900 h represented in Fig. 6 show more distortion compared to the leakage current measured at 500 h of experimentation. Figures 4, 5, 6 show the leakage current was only due to the surface resistance of the silicone rubber.

No significant changes were observed in the RMS values of the leakage current. Under normal/dry conditions below freezing point temperature, formation of water droplets is very remote. The current waveforms indicate some noise, but these noise signals may be due to source noise or due to interference or due to voltage fluctuations. This noise cannot be attributed to any activity and can be observed commonly in the case insulators like dry-band arcing and water droplet corona. It is thought that under applied experimental conditions, surface degradation may not happen for a very long period.

Further, it was felt that we need to understand the performance of insulators for sub-zero with polluted/

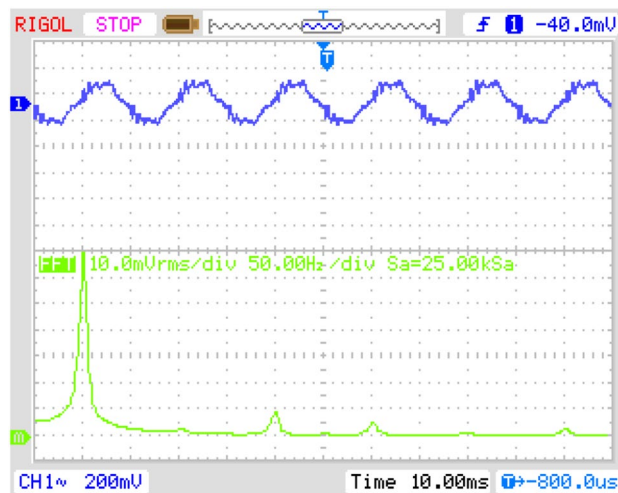


Fig. 7 Leakage current just after pollution and energizing

contaminated conditions. After 960 h of experimentation, two out of the four insulators under investigations were removed and polluted as per IEC 60507 [32] standards and investigated for $-20\text{ }^{\circ}\text{C}$. The pollution performance was continuously monitored and evaluated.

Figure 7 shows the leakage current measured immediately after applying the pollution slurry, while Fig. 8 shows the measured leakage current after about 547 h of experimentation. In both the cases the value of current peak is nearly 10 microamps. The application of pollution has caused the peak current to increase in comparison with the earlier conditions. The higher current is due to the wet nature of the pollution slurry. This causes the evaporation of the water and formation of dry bands resulting in the

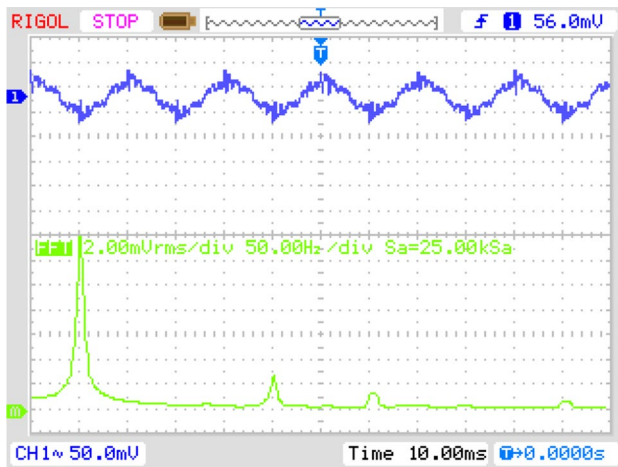


Fig. 8 Leakage current after 547 h of contamination at $-20\text{ }^{\circ}\text{C}$

formation of arcs. These arcs distort the current which can be seen from the FFT plot in Figs. 7 and 8, respectively.

The leakage current waveforms and the corresponding FFTs are important for interpretation as mentioned in [7], and the presence of various harmonics can indicate non-linear heating phenomenon occurring on the surface of the insulator. It is seen initially after the application of pollution the RMS value has increased, but this is momentary because the presence of wet conditions might have triggered water droplet corona along with dry-band arcing. The momentary increase in current may not indicate any significant loss of property like hydrophobicity.

The FFT waveforms of leakage current after application of the pollution show the presence of lower-level odd harmonics. This can be attributed to minor arcing phenomenon which may be occurring on the surface of the insulator [7].

Apart from the dry-band arcs causing the leakage current to distort, influence from the discharges arising near the triple-point singularity may also contribute. Any form of arcing phenomenon will make the waveform symmetrical; hence, it can be inferred that in case of normal/non-polluted conditions the source of harmonics is mainly discharges at the triple point and source harmonics. After application of the pollution layer, the magnitude of the leakage current has increased; this causes evaporation of water resulting in the formation of dry bands causing minor arcs superimposed on the leakage current, hence the generation of lower harmonic components, with progress in experimentation the increase in number of harmonics is not considerable. Figure 9 shows the graphical plot of the RMS values of four insulators: 1 and 2 are polluted after 960 h and 3 and 4 are non-polluted.

It is obvious from Fig. 9 that peak magnitude in the leakage current is due to the conduction of the pollution layer. As mentioned, the pollution slurry was applied only to insulator 1 and 2 and hence a sudden rise in the magnitude is observed

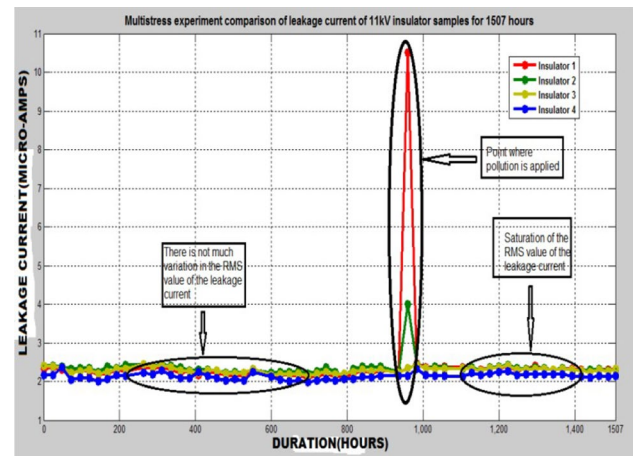


Fig. 9 Leakage current for total experimental duration

after 960 h. Later within few hours, the leakage current settles down to lower value. This has been consistent with the fact that pollution does not affect the surface degradation much.

The pollution layer dries up very quickly which causes the fall of the leakage current. In the dry climatic conditions, water droplets do not form on the surface. So, the chance of formation of a continuous conductive layer is very remote. From the leakage current measurements, analysis and also on the basis of available literature, it is obvious that surface degradation has not taken place on the unpolluted insulators. But the polluted insulators have undergone some degradation due to the dry-band arcing between the discontinuous pollution layers. This has been confirmed by the hydrophobicity measurements conducted as per IEC 62073 [33]. Figure 10 shows the pictures obtained showing water droplets accumulation on the surface after the completion of the experimentation.

Figure 10a–d is compared with the standards to obtain wettability class measurement as shown in Table 1.

From the wettability class measurements, it is seen that two insulators 1 and 2 for which pollution was applied have degraded to WC5. This is due to the dry-band arcing phenomenon occurring after the application of the pollutant causing the degradation. The phenomenon of surface discharge and its impact on the insulator surface has been lucidly dealt in the literature [2, 4, 5, 8]. Further, to understand the degradation in detail FTIR and SEM analyses on the insulators are conducted, and results are analyzed and presented.

4 Fourier transform infrared spectroscopy (FTIR) on aged samples

FTIR studies have been conducted to understand the material degradation at the microscopic level for the aged samples under 0° and $-20\text{ }^{\circ}\text{C}$. The FTIR is conducted using

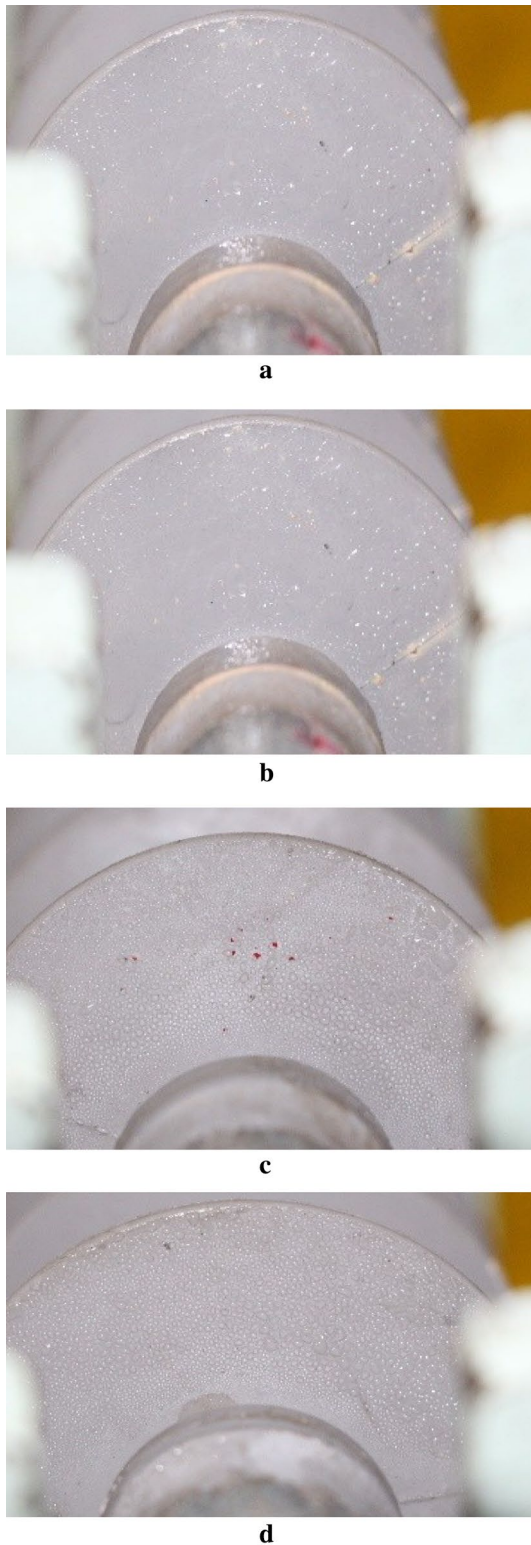


Fig. 10 Water droplets on **a** insulator1 **b** insulator2 **c** insulator3 **d** insulator4

Table 1 Measurement of wettability class for insulators

Insulator 1	WC-5
Insulator 2	WC-5
Insulator 3	WC-2
Insulator 4	WC-2

PerkinElmer make MIR spectrometer with attenuated total reflection (ATR) equipped with the diamond crystal. As observed the leakage current may be an indicator about various thermal phenomena like arcing that may have taken place along the insulator surface, but the material degradation can only be indicated by various material testing analysis at microscopic level. The samples are initially tested at zero °C under low humidity conditions. Later, new samples are experimented for $-20\text{ }^{\circ}\text{C}$ to see the effect of extreme cold climatic conditions on the material properties composite insulators. FTIR plots are described based on John and Paul [34].

Figure 11 shows the FTIR plot of the samples aged under the 0° cold climate with electrical stress. The period of experimentation was 1000 h. It is observed from the FTIR plot for the range $3700\text{--}3500\text{ cm}^{-1}$ that minor change is observed; this change is due to the silanol that is formed in the aged samples due to slight oxidation effect. The oxidation effect can be accounted due to the discharges that may have originated from the triple junction of the insulator, air and the metal fitting that are simultaneously present. Under dry condition the possibility of discharges taking place is very remote, the main chain breakage seen in Fig. 11 is also insignificant. Thus, the FTIR analysis at 0° conditions does

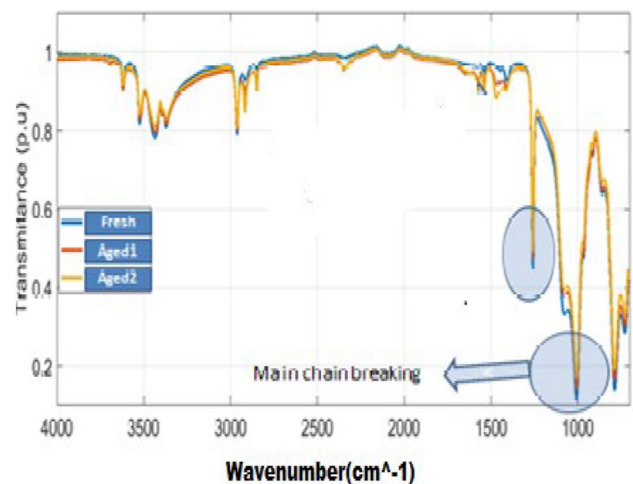


Fig. 11 FTIR analysis of aged and fresh sample after 1000 h of experimentation under 0° temperature and electrical stress

not exhibit degradation on the material surface and not much change was observed in leakage current waveforms for a period of 1500 h of experimentation due to the dry and low humid conditions.

Further, to assess the material degradation on the samples aged under -20° with application of pollution on the surface, experimentation was conducted, and the analysis is presented. The FTIR analysis is conducted on the shed which is near to the high-voltage electrode and on the shed near the ground end, and on the polluted insulators.

4.1 FTIR analysis and discussion on polluted insulator samples under sub-zero conditions

The polluted and non-polluted insulators are compared based on the FTIR analysis, and the top shed (shed near the HV end) and bottom shed (near the ground end) are considered for analysis. For brevity results of insulator 2 (polluted) and insulator 3 (not polluted) are chosen for comparative analysis.

From Fig. 12 it is seen that for polluted insulator 2, there is a considerable distinction between the plots of the top shed and bottom shed. The band $3500\text{--}3700\text{ cm}^{-1}$ refers to the interacting --OH (hydroxyl) group, and the band $3200\text{--}3500\text{ cm}^{-1}$ refers to the non-interacting --OH group. The intensity of this region for top shed is comparatively less compared to the bottom shed. Moreover, the --Si--CH_3 symmetrical stretching peak is also less for the top shed which is approximately located at 2961 cm^{-1} (Fig. 13).

Similarly, the --Si--C vibration peak at 1261 cm^{-1} is less intense for the top shed compared with the bottom shed. The band from $900\text{ to }1200\text{ cm}^{-1}$ refers to the main chain --Si--O--Si-- stretching. The intensity peak for the insulator 2 top shed is less compared to the bottom shed. But for the non-polluted insulator 3 the main bands pertaining to PDMS almost overlap. This kind of behavior is mainly due to the dry-band discharges taking place more intensely at the high-voltage end

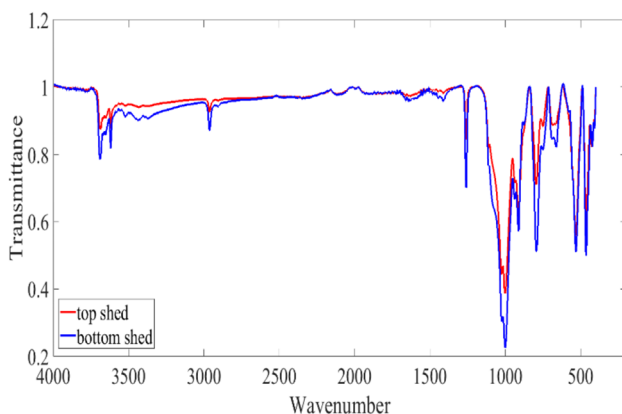


Fig. 12 FTIR of insulator 2 conducted after 1250 h

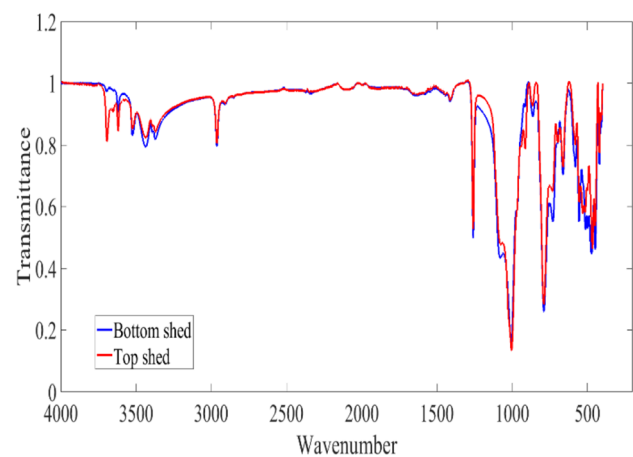


Fig. 13 FTIR of insulator 3 conducted after 1250 h

compared to the ground side. The intensity of the discharge is severely increased after the application of the pollution.

This is explained based on the fact that the electric field near the high-voltage electrode is increased due to the singularity effect at the triple junction, and the dry-band arcing taking place near the high-voltage electrode is more severe. The strong ionization of the medium and the bombardment of ions on the SIR surface could be reason as seen from the FTIR plot of the insulator 2, and the --OH peaks both for interacting and non-interacting --OH are less for the top shed compared to the bottom shed. Moreover, the --Si--CH_3 peak and --Si--C peak are also reduced. The reason for such an observation is as follows: due to the high intensity of the dry-band arcing near the top shed of the insulator, the --Si--CH_3 is oxidized to the --Si--OH (silanol group) but these silanol compounds will again cross-link to form silica which will make the surface rough. Even though silanol is produced, the --OH peak due to interacting moisture is reduced due to the generation of silica which is indicated in the SEM results.

Moreover, the intensity of the peak due to non-interacting moisture of the filler ATH has three molecules of water of crystallization seen to have decreased. This is because the water molecules of crystallization are evaporated from the surface. The other peak which is seen is the FTIR plot of insulator 2 is the effect on the main chain (--Si--O--Si--), the intensity of this band is less for the top shed compared to the bottom shed, and this might have happened due to the main chain breaking reactions which are severe at the high-voltage end may have initiated. For insulator 3 there is no considerable effect on the dry-band discharges as the top shed, in the FTIR plot is observed to overlap with the bottom shed plot. It is evident that as the pollution increases the severity of the dry-band discharges and its impact is intensified due to the electric field increasing at the triple point near the HV electrode.

FTIR conducted after 1507 h (end of experiment) is shown in Fig. 14 for insulator 2, and observations remain the same, but rate of degradation is rapidly increased due to the long exposure of top shed to dry-band discharges. Moreover, the peak due to $-OH$ in ATH is almost flat indicating water of crystallization of ATH is evaporated causing the insulation to degrade more on the SIR surface. In addition, the intensity of the main chain peak is considerably low for top shed compared to the bottom shed. This is an indication that most severe degradation takes place at the high-voltage end and intensity decreases toward the ground end.

Figures 15 and 16 show the FTIR spectrum for four insulators. For the bottom sheds, the $-OH$ band in 3200 cm^{-1} to 3500 cm^{-1} is attributed to the water of crystallization present in ATH shows more intense peak for non-polluted insulators but not present in the polluted insulators. The effect of heating due to dry-band discharges can be seen in the polluted insulators. The heat from the dry-band discharges is enough to cause the water to evaporate.

Another important observation from Figs. 15 and 16 is that $-OH$ interacts and is present in the form of silanol producing more intense peaks for bottom sheds of polluted insulators compared to the non-polluted insulators. On the contrary, for top sheds for polluted insulators the effect of silanol shown is almost removed. This effect is due to the oxidation of methyl group attached to the main chain, and silicone produces silanol which under dry-band arcing forms silica.

The dry-band impact on the bottom sheds produces only silanol which after enough time may transform into silica. Due to the severity of the dry-band arcing on top shed of the polluted insulator, the formation of silica is seen only after 350 h after the application of pollution. The significant band for study is the $1130\text{--}1000\text{ cm}^{-1}$ as this represents the main chain characteristics that are $-\text{Si}-\text{O}-\text{Si}-$. For the PDMS compound, there will be two peaks in this region.

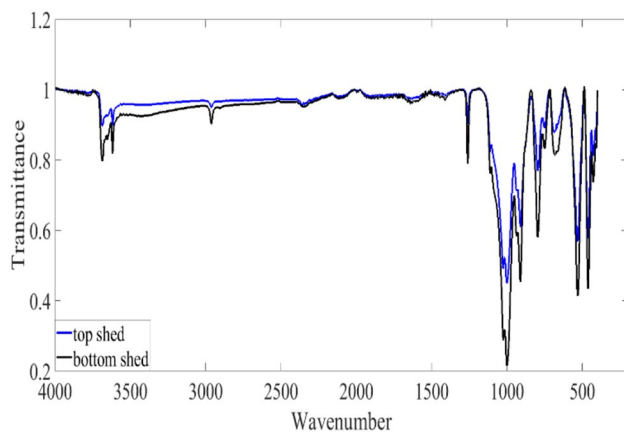


Fig. 14 FTIR of insulator 2 conducted after 1507 h

Di-siloxanes and small-ring siloxanes show only a single sharp peak in this band. But as the PDMS chain becomes broader, the chain becomes more complex as indicated in two peaks in the infrared spectroscopy results. The FTIR plots show polluted insulators have two peaks present, but the intensity of the peaks is not sharp as those of non-polluted insulators.

For the top shed the peak is almost converging at 1000 cm^{-1} after 350 h of application of pollution. This is indicative of the fact that main chain breaking is taking place as the time of application of pollution. This chain breaking can be attributed to the dry-band arcing which may have started after application of the pollution. But the non-polluted insulators are showing both peaks in this band ($1130\text{--}1000\text{ cm}^{-1}$) because no such arcing phenomenon has occurred.

Figure 17 shows the FTIR plot conducted on the bottom sheds; comparing this with Fig. 16 the following facts are observed. The two peaks due to the $-\text{Si}-\text{O}-\text{Si}-$ do exist in

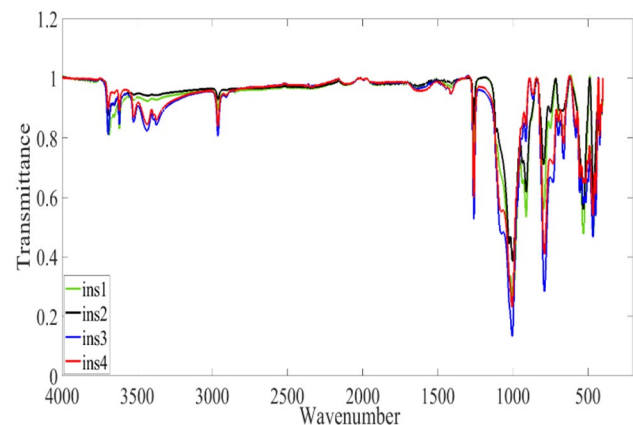


Fig. 15 FTIR of all insulators' top sheds conducted after 1250 h

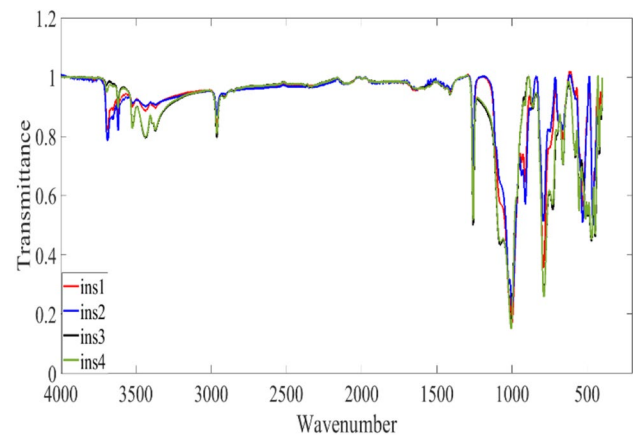


Fig. 16 FTIR of all insulators' bottom shed conducted after 1250 h

the polluted insulators after 350 h of polluting or 1250 h of experimentation (pollution was applied after 950 h of the experiment); at the end of experiment, the peaks almost converge to a single peak at approximately 1000 cm^{-1} . Thus, with time the degradation with respect to main chain breaking increases.

From Fig. 18 it is observed that the insulator 2 is heavily degraded after the end of experiment. The relevant peaks for $-\text{Si}-\text{CH}_3$ and main chain ($-\text{Si}-\text{O}-\text{Si}-$) have shown a significant decrease in the intensity.

As observed from the FTIR plots (Figs. 15, 16, 17, 18), the main chain siloxane is converging at the vicinity of 1000 cm^{-1} and this is due to main chain breaking and generation of low molecular weight species of PDMS. As observed in literature [2, 5], the LMW species help in recovery of the lost hydrophobicity. During wettability experimentation, it was seen that the polluted insulators fall into WC-5 while the non-polluted insulators belong to WC-2. The reasons could be the following: Firstly, formation of silica on the polluted silicone rubber insulators hinders the movement of LMW chains to the surface. Secondly, the boiling points of LMW chains are low and so they have vaporized from the surface and thus the hydrophobicity could not be restored. This is because dry-band discharges have occurred after application of the pollution. It was seen in the leakage current analysis that rms values of the leakage current did not change considerably over the period. Moreover, under thermal degradation the LMW chains have moved to the surface and the hydrophobicity could have been restored. The dry-band arcing of polluted insulators under cold and dry conditions may cause severe material damage as seen from the FTIR analysis. The dry-band arcing after application of pollution till the time of the evaporation during this interval degradation has been severe, and hence, the changes in the FTIR plots are observed.

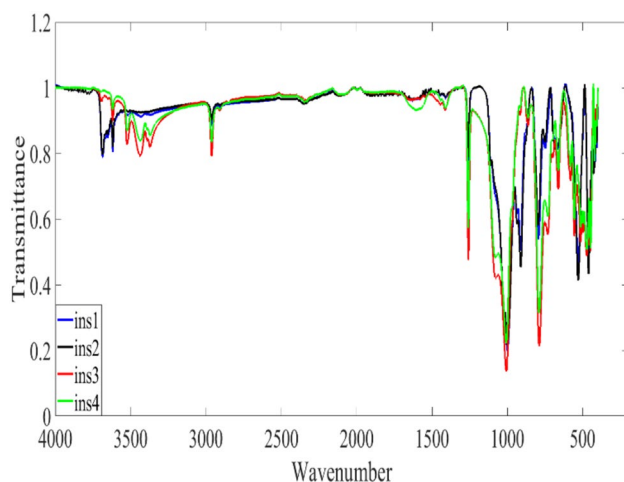


Fig. 17 FTIR of all insulators' bottom shed conducted after 1507 h

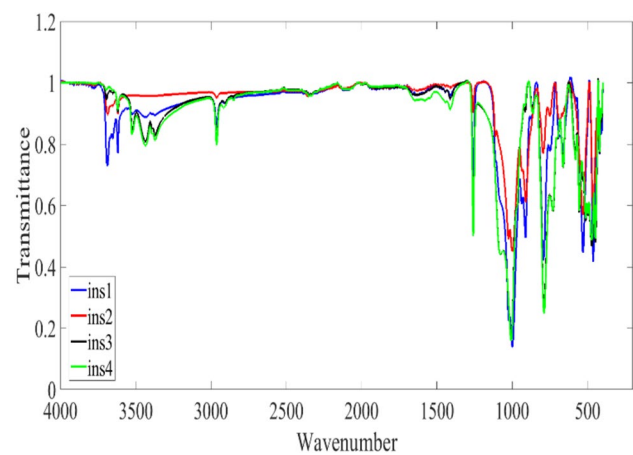


Fig. 18 FTIR of all insulators' top shed conducted after 1507 h

5 SEM and EDX of aged samples

SEM and EDX studies are conducted on aged samples and are compared with the fresh sample at zero and -20° .

The SEM image shown in Fig. 19 is for 0° at low humidity (35%); it is observed from the figure that after 1000 h some minor degradation is noticed on the sample. Figures 20, 21, 22, 23 show the images of SEM after the experimentation at -20°C . The smoother the surface appears, the lesser the breaking of main chain is. Appearance of ATH on the surface due to the dry-band arcing, partial silanol formation and cross-linking forming silica renders the surface as seen from the SEM results. The SEM results are compared for insulator 1 (which is polluted) and insulator 4 (the unpolluted one). The SEM has been conducted on the insulator 1 for the top shed (near the HV end) and the bottom shed near the ground end. The top shed and the bottom shed are exposed to different levels of electric field, and hence, the degradation level

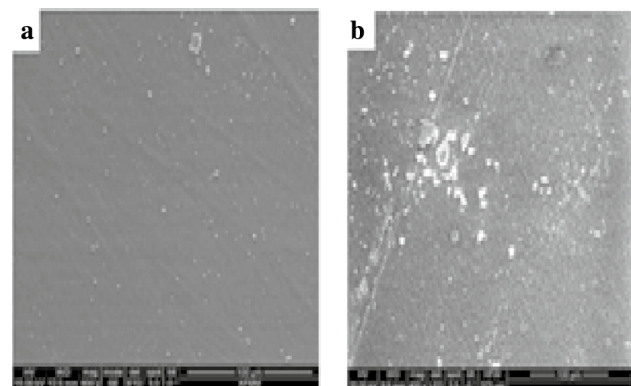


Fig. 19 SEM of the insulators **a** fresh sample **b** treated sample after 1000 h at 0°C

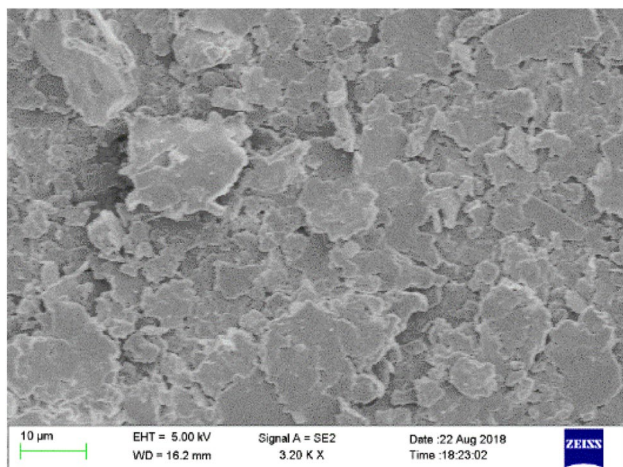


Fig. 20 SEM picture of the bottom shed of insulator 1 after 1507 h of experimentation under sub-zero conditions

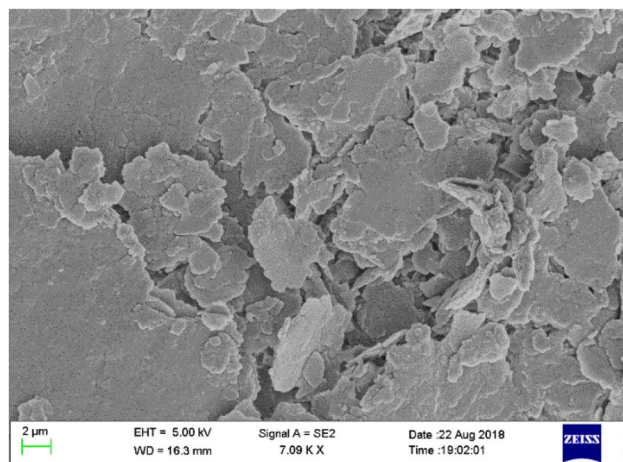


Fig. 21 SEM picture of the top shed of insulator 1 after 1507 h of the experimentation under sub-zero conditions

due to dry-band arcing will also be different, and this is the reason for the SEM images to be different.

Figure 20 shows the SEM image of the bottom side of insulator 1, the SEM image shows several cracked portions, and this appearance is due to the dry-band arcing which occurred after the application of the pollution layer.

Figure 21 shows the SEM results of the same insulator for the top shed portion. More degradation is observed; this may be due to the discharges arising from triple point contributing in the higher degradation of the shed, as it happens to be near the high-voltage electrode.

SEM image in Fig. 22 and 23 is shown for non-polluted insulator 4. The bottom shed which is nearer to the ground end shows almost a smooth surface but the top shed which is very close to the high-voltage electrode gives a chalky

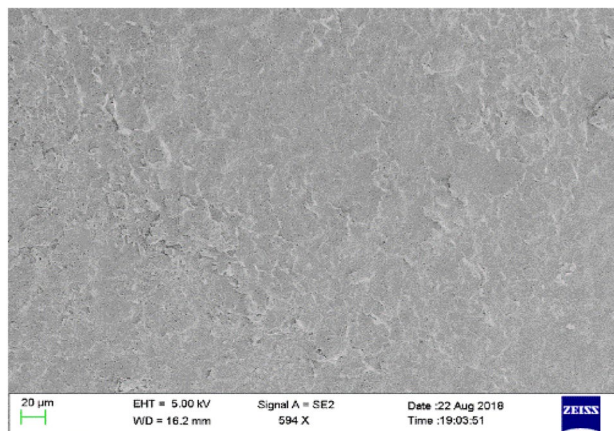


Fig. 22 SEM picture of the bottom shed of insulator 4 after 1507 h of experimentation under sub-zero conditions

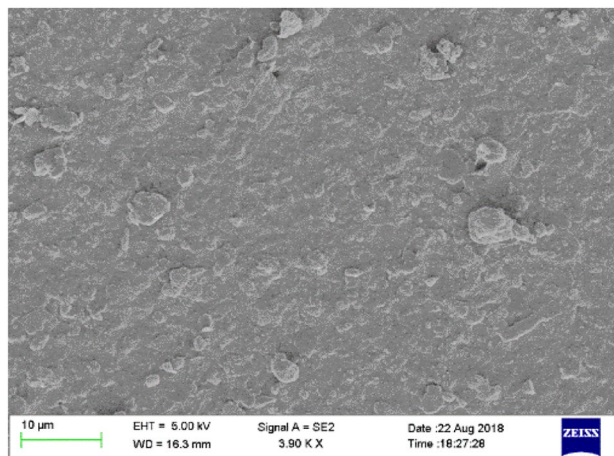


Fig. 23 SEM picture of the top shed of insulator 4 after 1507 h of the experimentation under sub-zero conditions

appearance. It is seen that the appearance of rough surface is not severe as in case of insulator 1 (Figs. 20 and 21). Therefore, the following observations are made from the SEM study: the effect of pollution on the insulators has shown more degradation and application of pollution enhances the dry-band activity which has triggered severe surface degradation on the polymeric surface.

The dry-band arcing on the polluted insulators has started after application of pollutant in the wet stage, and the dry conditions are restored and less severe activity like triple-point emissions started taking place later. The second observation is the effect of triple-point arcing near the high-voltage electrode which has caused the surface even in unpolluted case to develop a chalky appearance (Fig. 23). The chalky appearance on the top shed of insulator 4 is due to the formation of silica due to the

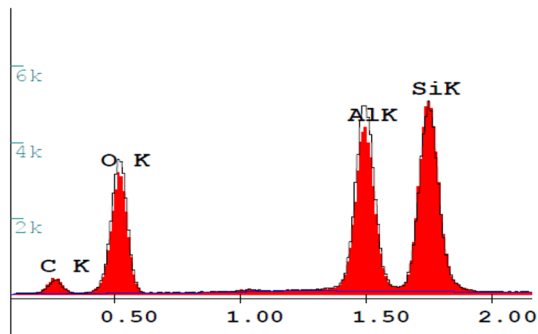


Fig. 24 EDAX of the sample after 1000 h (in black) and fresh sample (in red) (x-axis in keV and y-axis in Counts)

cross-linking of the silanol groups. The SEM study correlates with the FTIR analysis.

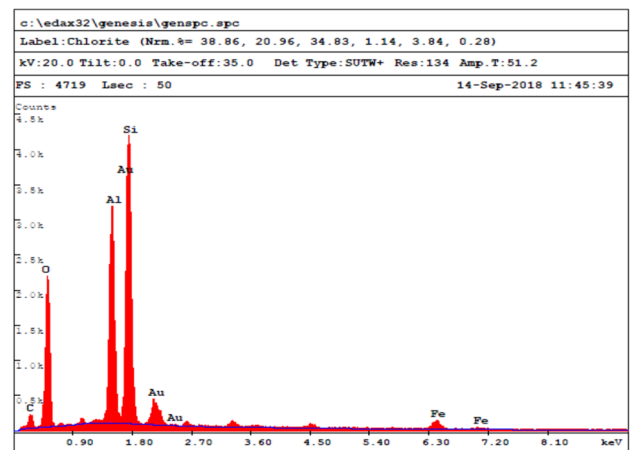
The EDAX analysis on the samples was conducted for Zero and $-20\text{ }^{\circ}\text{C}$. Figure 24 shows the elemental composition on the surface of insulators after 1000 h of experimentation at 0° . The analysis of fresh sample is shown by the red peaks, while the treated sample is shown by the black peaks. From the figure it is seen that for the treated sample the oxygen level has increased marginally. This may be due to the oxidation which has taken place along the surface of the insulators.

The oxidation could have resulted in the appearance of white spots on the material surface as seen in the SEM images (Fig. 19). Aluminum level has also increased; this may be due to the ATH filler which may have come to the surface due to occurrence of thermal phenomenon. The sample for the EDAX and SEM is taken from the top shed which is near the triple junction. The observations from SEM to EDAX show not much of degradation on the material surface due to the cold climate and low humidity. Further investigations have been extended to $-20\text{ }^{\circ}\text{C}$ to understand the performance wherein some parts of the country witness this temperature during winter with low humidity levels.

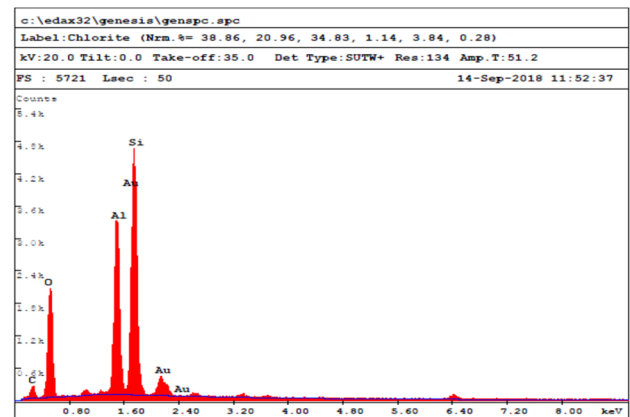
The EDAX analysis on the samples was conducted after completion of the 1507 h. of the experimentation. The insulators which are polluted include insulator 1 and 2. The other insulators (3 and 4) are only studied under non-polluted condition to see the impact of sub-zero temperature and electrical stress.

As seen from Figs. 25 and 26, the surface degradation of the insulator 2 is comparatively higher than that of insulator 1. The higher silicone level in insulator 2 is indicative of the higher presence of silica. This silica is formed due to cross-linking of the silanol compounds. Moreover, the amount of elemental aluminum is more in the insulator 2 surface (top shed) compared to that of insulator 1 (top shed).

This phenomenon may be due to the dry atmosphere the possibility of thermal phenomenon (like dry-band arcing



a



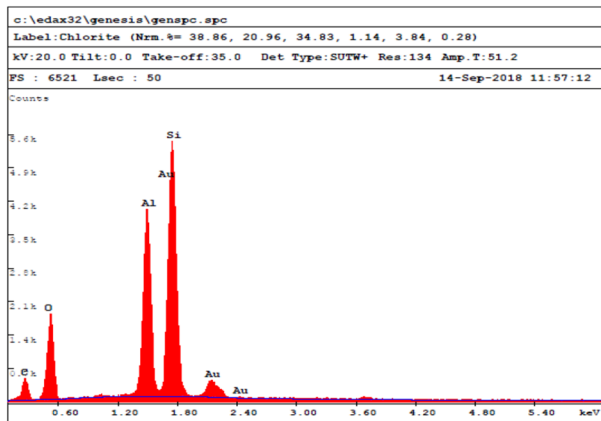
b

Fig. 25 a EDAX of the bottom shed of insulator 1 and **b** EDAX of the top shed of insulator 1 (x-axis in keV and y-axis in Counts)

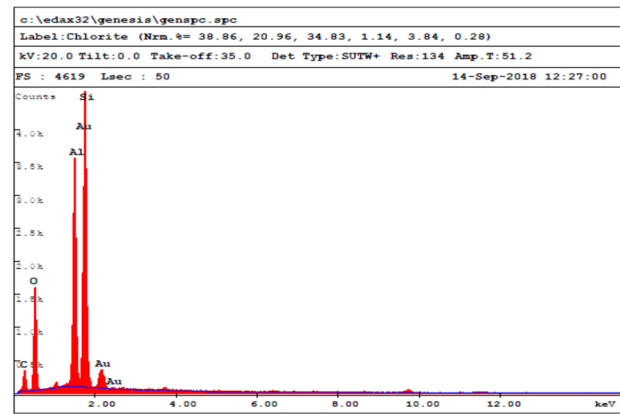
etc.). The severity of discharges at the triple point near insulator 2 high-voltage electrode can be justified by comparing Fig. 25a, b. Figure 25 shows the insulator 1 top shed and bottom shed are shown. The relative amounts of the elements (silicone, aluminum, oxygen) are almost same.

This confirms that the severity of the discharges in case of insulator 1 are weak to cause significant damage to the top shed compared to the bottom shed. Comparing Fig. 26a, b the intensity of the discharges near the high-voltage electrode is significant enough to cause considerable changes on the surface. The amount of aluminum is higher on the top shed of insulator 2 less on the bottom shed; moreover, the amount of silicone is also more.

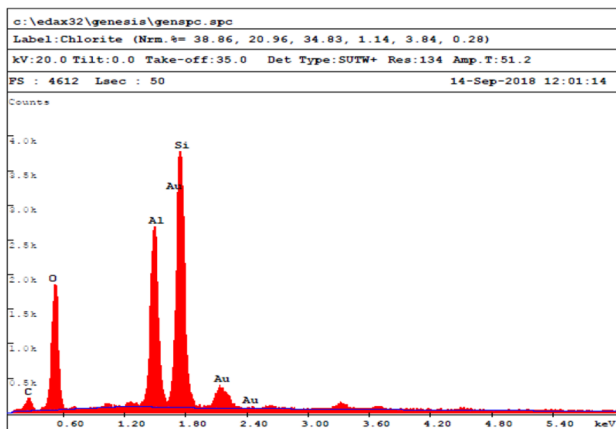
The quantity of aluminum in both insulator 3 and 4 are almost same as indicated in Fig. 27; however, the amount of silicone and oxygen is more in case of insulator 3. In Insulator 3 the amount of carbon is less compared to insulator 4. This explains that the intensity of discharges near the high-voltage electrode is much more severe in case of insulator 3 compared to insulator 4. The formation of silica by



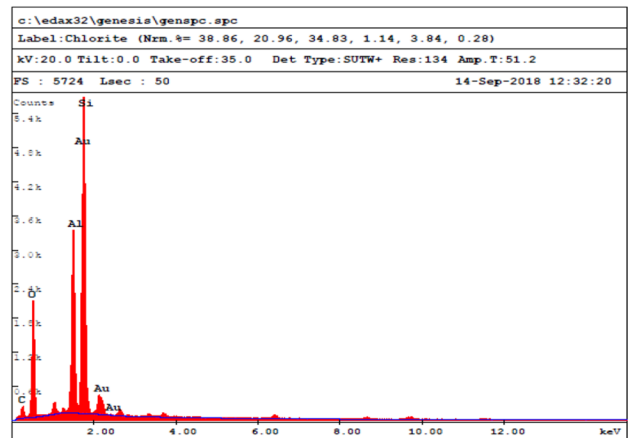
a



a



b



b

Fig. 26 a EDAX of bottom shed of insulator 2 b EDAX of Top shed of insulator 2 (x-axis in keV and y-axis in Counts)

Fig. 27 a EDAX of bottom shed of insulator 3 b EDAX of top shed of Insulator 4. (x-axis in keV and y-axis in Counts)

cross-linking of silanol is indicative of the fact that the thermal discharges has oxidized the methyl group to hydroxyl group resulting in the formation of silanol (hence a reduction in carbon peak) and the cross-linking of the silanol groups has resulted in the formation of silica (increase in the silicone and oxygen).

Comparing the results of zero and sub-zero conditions, it can be inferred that application of pollution has resulted in the considerable degradation. The pollution layers may have been dried, but the local conductivity at different places on the insulator surface is different resulting in the non-uniform distribution of surface current. Local temperature at some places may be very high, while at some places may be comparatively low. Distribution of pollution and its effect on the distribution of surface current can significantly affect the surface elemental composition.

Earlier for 0° the comparison was done with the fresh sample and results presented show that the degradation of the surface is insignificant. This experiment later motivated us to proceed with sub-zero temperature. Here we have used

two types of comparison, firstly the top and bottom sheds of the insulators were compared. This is done to clearly access the effect of discharges from the high-voltage electrode. Later, we used the comparison between the polluted and non-polluted insulator to see the effect on the performance. The comparative results presented clearly indicate the fact that for efficient condition monitoring under cold climate analyzing the samples under different temperature, electric stress along with various environmental conditions are required.

6 Tensile strength measurements

The tensile strength measurements were conducted on the dumbbell-shaped specimen by stretching the sample in the test machine until it breaks as per IS 3400 [35]. The amount of force required to break the material in tension and extent to which specimen stretches or elongates to the breaking point are measured. Stress–strain measurements are performed with Intron 5967 screw driven Universal Testing

Table 2 Elongation break percentage reduction at various temperatures

Temperature (°C)	% reduction in elongation
0	8
−20	24

Machine (UTM) with load capacity of 30 KN at cross-head speed of 200 mm/min. Measurements are conducted for various temperature and electric stress, and a comparison is shown in Table 2. It is observed that elongation break percentage is more at higher temperature and reduces to significant values at lower temperature; elongation break percentage seen is 24% reduction at −20 °C and 8% at 0 °C. With temperature decreasing below 0 °C, the ductile nature of the silicone rubber is found to decrease.

7 Conclusions

The experimental investigations were conducted at zero and sub-0° temperature conditions to understand the impact of very low temperature on the insulator performance. In the sub-zero temperature experimentation, the impact of pollution is also studied. The investigations conducted simulate near real-time environmental conditions which exist in some parts of the country.

The leakage current was monitored throughout the experimental duration. It was seen the degradation is minimal, the leakage current observed is almost sinusoidal, and minor degradation (or oxidation of the side chain methyl group) was noticed on the insulator performance at 0° under dry condition

Further, experimentation was conducted at −20° under normal and with polluted conditions. Results indicated that degradation present on the top shed is much more compared to the bottom shed. The FTIR plots show considerable differences in the level of degradation more on the top sheds near HV compared to the bottom sheds.

Similar results were seen with the EDAX analysis where the aluminum level on the top shed for the polluted insulators was higher compared to that at the bottom sheds. This is indicator to the fact that the intensity of thermal activity on the top shed is much higher compared to that of the bottom shed. Basically, the top sheds are exposed to higher intensity discharges compared to the bottom shed due to it being nearer to the high-voltage electrode.

With pollution the degradation is aggravated due to the local intensification of the current at some points. The discontinuous films of dry pollution layer trigger faint discharges, which are reflected in the FFT plots as low peaks compared to the much higher fundamental.

The tensile stress measurements show under cold climate (sub-zero) condition the material becomes brittle and hence the tendency to break is increased. The reduction in the tensile strength is a clear indicator that significant changes have occurred on the surface of Insulating material.

Acknowledgements Authors are grateful to SERB-DST, Govt of India, for financial assistance under SERB No: EEQ/2016/000030 and also thankful to Mr. Kiran of M/s Goldstone Insulators, Hyderabad, India, for the help and encouragement.

References

- Gorur RS, Cherney EA, Burnham JT (1999) Outdoor Insulators. Ravi S Gorur Inc.
- Papailiou KO, Schmuck F (2013) Silicone composite insulators materials, design, applications. Springer, Berlin
- Hackam R (1999) Outdoor HV composite polymeric insulators. IEEE Trans Dielectr Electr Insul 6:557–585
- Kumagai S, Yoshimura N (2000) Impacts of thermal aging and water absorption on the surface electrical and chemical properties of cycloaliphatic epoxy resin. IEEE Trans Dielectr Electr Insul 7(3):424–431
- Yoshimura N, Kumagai S, Nishimura S (1999) Electrical and Environmental aging of Silicone rubber used in outdoor insulation. IEEE Trans Dielectr Electr Insul 6:632–650
- Ilhan S, Cherney EA (2018) Comparative tests on RTV silicone rubber coated porcelain suspension insulators in a salt-fog chamber. IEEE Trans Dielectr Electr Insul 25:569
- El-Hag AH, Jayaram SH, Cherney EA (2003) Fundamental and low frequency harmonic components of leakage current as a diagnostic tool to study aging of RTV and HTV silicone rubber in salt-fog. IEEE Trans Dielectr Electr Insul 10:128–136
- Meyer LH, Cherney EA, Jayaram SH (2004) The role of inorganic fillers in silicone rubber for outdoor insulation alumina tri-hydrate or silica. IEEE Electr Insul Mag 20:13–21
- Phillips AJ, Childs DJ, Schneider HM (1999) Aging of non-ceramic insulators due to corona from water drops. IEEE Trans Power Deliv 14(3):665
- Shah M, Karady G, Brown RL (1995) Flashover mechanism of silicone rubber insulators used for outdoor insulation—II. IEEE Trans Power Deliv 10(4):1972–1978
- George G, Karady T (1999) Flashover mechanism of non-ceramic insulators. IEEE Tans Dielectr Electr Insul 6(5):598
- El-Kishky H, Gorur RS (1996) Electric field computation on an insulating surface with discrete water droplets. IEEE Trans Dielectr Electr Insul 3(3):450–456
- Schneider HM, Guidi WW, Burnham JT, Gorur RS, Hall JF (1993) Accelerated aging and flashover tests on 138 kV nonceramic line post insulators. IEEE Trans Power Deliv 8(1):325–336
- Venkatesulu B, Thomas JM (2007) Long-term accelerated multi-stress aging of composite outdoor polymeric insulators. In: 2007 International conference on solid dielectrics, Winchester, UK
- Raji S, Esaki S, Areef M, Jason G (2006) Multistress accelerated aging of polymer housed surge arresters under simulated coastal Florida conditions. In: IEEE transactions on dielectrics and electrical insulation vol 13, no 1
- Chemey EA, Stonkus DJ (1981) Non-ceramic insulators for contaminated environments. IEEE Trans PAS 100:131–142
- Farzaneh M (2014) Insulator flashover under icing conditions. IEEE Trans Dielectr Electr Insul 21(5):5698

18. Farzaneh M, Chisholm WA (2009) *Insulators for icing and polluted environments*. Wiley, New York
19. Ghosh P, Chatterjee N (1995) Polluted insulator flashover model for AC voltage. In: *IEEE transactions on dielectrics and electrical insulation*, vol 2, no 1
20. Cheng TC, Jolly DC, King DJ (1977) Surface flashover of water repellent insulators under moist conditions. *IEEE Trans Electr Insul* 12(3):759
21. Wilkins R (1969) Flashover voltage of high-voltage insulators with uniform surface-pollution films. *Proc IEE* 116(3):457–465
22. Rahul C, Subba RB (2017) Studies on high temperature vulcanized silicone rubber insulators, under arid climatic aging. *IEEE Trans Dielectr Electr Insul* 24(3):1751–1760
23. Alok RV, Subba RB (2017) Accelerated aging studies of silicon-rubber based polymeric insulators used for HV transmission lines. *J Polym Test* 62:124–131
24. Alok RV, Subba RB, Rahul C (2018) Multistress aging studies on polymeric insulators. *IEEE Trans Dielectr Electr Insul* 25(2):524–532
25. Alok RV, Subba RB (2018) Aging studies on polymeric insulators under DC stress with controlled climatic conditions. *J Polym Test* 68:185–192
26. Dinesh S (2018) Studies on high voltage composite insulators under multiple stresses, M.Sc thesis, Department of Electrical Engineering, Indian Institute of Science, Bangalore
27. Dinesh S, Subba RB (2018) Studies on high voltage composite insulators under very low temperature. In: *IEEE international conference on high voltage engineering and application*, ICHVE 2018
28. Li Shengtao, Shihu Yu, Feng Yang (2016) Progress in and prospects for electrical insulating materials. *IET High Volt* 1(3):122–129
29. Mehmet MI, Aysel EY, Özcan K (2018) Investigation of tracking phenomenon in cable joints as 3D with finite element method. *Electr Eng* 100:2193–2203
30. Banik Apu, Mukherjee Abhik, Dalai Sovan (2018) Development of a pollution flashover model for 11 kV porcelain and silicon rubber insulator by using COMSOL Multiphysics. *Electr Eng* 100:533–541
31. Barzegaran MR, Mohammed OA (2018) Condition monitoring of power components in electric grid using electromagnetic stray fields. *Electr Eng* 100:499–508
32. IEC 60507 (2013) Artificial pollution tests on high-voltage ceramic and glass insulators to be used on AC systems
33. Guidance on the measurement of wettability of insulator surfaces. In: *IEC/TS 62073*, Tech Report, 2003(E)
34. John PC, Paul HS (2009) *Infrared spectroscopy in process analysis*. Wiley, New York
35. Methods of test for vulcanized rubber part 1 determination of tensile stress-strain properties. *IS 3400-1*

Publisher's Note Springer Nature remains neutral with regard to jurisdictional claims in published maps and institutional affiliations.